Prolonged low-dose dioxin exposure impairs metabolic adaptability to high-fat diet feeding in female but not male mice

Geronimo Matteo[1]*, Myriam P Hoyeck[1]*, Hannah L Blair[1], Julia Zebarth[1], Kayleigh RC Rick[1], Andrew Williams[2], Rémi Gagné[2], Julie K Buick[2], Carole L Yauk[2,3], Jennifer E Bruin[1#].

* Authors contributed equally

[1]Department of Biology & Institute of Biochemistry, Carleton University, Ottawa, Ontario, K1S 5B6 Canada.

[2] Environmental Health Science and Research Bureau, Health Canada, Ottawa, Ontario K1A 0K9 Canada.

[3]Department of Biology, University of Ottawa, Ontario, KIN 6N5

[#] Address correspondence to:
Dr. Jennifer Bruin
244 Nesbitt Biology Building
1125 Colonel By Drive
Ottawa, ON K1S 5B6
T: 613-520-2600 x3656
jenny.bruin@carleton.ca

Abstract:

Objective: Human studies consistently show an association between exposure to persistent organic pollutants, including 2,3,7,8-tetrachlorodibenzo-*p*-dioxin (TCDD, aka "dioxin"), and increased diabetes risk. We previously showed that acute high-dose TCDD exposure (20 µg/kg) decreased plasma insulin levels in both male and female mice *in vivo*; however, effects on glucose homeostasis were sex-dependent. The purpose of this study was to determine whether prolonged exposure to a physiologically relevant dose of TCDD impairs beta cell function and/or glucose homeostasis in a sex-dependent manner in either chow-fed or HFD-fed mice.
Methods: Male and female mice were exposed to 20 ng/kg/d TCDD 2x/week for 12 weeks, and simultaneously fed a chow or 45% high-fat diet (HFD). Glucose metabolism was assessed by glucose and insulin tolerance tests throughout the study. Islets were isolated from females at 12 weeks for Tempo-Seq® analysis.
Results: Low-dose TCDD exposure did not lead to adverse metabolic consequences in chow-fed male or female mice, or in HFD-fed males. However, TCDD accelerated the onset of HFD-induced hyperglycemia and impaired glucose-induced plasma insulin levels in female mice. In addition, islet TempO-Seq® analysis showed that TCDD exposure promoted abnormal changes to endocrine and metabolic pathways in HFD-fed females.
Conclusions: Our data suggest that TCDD exposure is more deleterious when combined with HFD-feeding in female mice, and that low-dose TCDD exposure increases diabetes susceptibility in females.

Keywords: beta cells, diabetes, dioxin, hyperglycemia, insulin, sex differences

Abbreviations

AhR	Aryl hydrocarbon receptor
CO	Corn oil
Cyp1a1	Cytochrome P450 1A1
DEG	Differentially expressed gene
GTT	Glucose tolerance test
HFD	High-fat diet
ITT	Insulin tolerance test
POPs	Persistent organic pollutants
TCDD	2,3,7,8-tetrachlorodibenzo-*p*-dioxin

1. Introduction

Global diabetes incidence is on the rise, yet the underlying causes for this increase remain to be elucidated (1). Type 2 diabetes is the most common form of diabetes, and is characterized by chronic hyperglycemia, insufficient insulin production by pancreatic beta cells, and peripheral insulin resistance (2). Genetics and lifestyle factors, such as physical inactivity and poor diet, are known risk factors for type 2 diabetes (2). However, these risk factors alone cannot account for the rapid increase in diabetes burden.

Persistent organic pollutants (POPs) are concerning environmental contaminants since they resist degradation and bioaccumulate. High serum POP concentrations are positively associated with a modest relative risk of developing diabetes (3–8) and insulin resistance (9,10) both in the general population with chronic low-dose POP exposure (11–13) and in individuals with high-dose exposure (e.g. veterans, chemical disaster victims, and occupational workers) (14–16). Most epidemiological studies investigating the association between POP exposure and diabetes risk only report male data. Interestingly, the few studies that considered both sexes suggest the positive correlation between POP serum concentrations and diabetes risk is greater in females. For example, follow-up studies on the Seveso population exposed to 2,3,7,8-tetrachlorodibenzo-*p*-dioxin (TCDD, aka "dioxin") found a higher relative risk of developing diabetes in females than males (15,17). In addition, high serum POP levels in the Michigan (18) and Yucheng (8) cohorts were associated with increased diabetes incidence in women only. A causal link between POP exposure and diabetes pathogenesis remains to be established, and potential sex differences require further investigation.

Dioxin/TCDD is a potent aryl hydrocarbon receptor (AhR) agonist and an excellent model chemical for investigating the relationship between dioxin-like compounds and diabetes risk. Although TCDD is now well regulated worldwide, there are hundreds of dioxin-like chemicals that remain a global concern for human health (19). We have shown that TCDD exposure induces AhR-regulated genes, including cytochrome P450 1a1 (*Cyp1a1*), in pancreatic islets, demonstrating that TCDD reaches the endocrine pancreas *in vivo* (20). Direct TCDD exposure also reduced glucose-stimulated insulin secretion in mouse and human islets *in vitro* (20). Interestingly, a single high-dose injection of TCDD (20 µg/kg) *in vivo* reduced plasma insulin levels in both male and female mice, but overall metabolic effects differed drastically between sexes (21). TCDD-exposed males had modest fasting hypoglycemia for ~4 weeks post-injection, increased insulin sensitivity, and decreased beta cell area compared to vehicle-exposed controls. Conversely, TCDD did not alter insulin sensitivity or islet composition in females, but induced transient hyperglycemia during a glucose tolerance test (GTT) at 4 weeks post-injection (21). Whether similar sex-specific effects occur with a physiologically relevant dose of TCDD remains to be investigated. Interestingly, we found that transient low-dose TCDD exposure (20 ng/kg/d, 2x/week) during pregnancy/lactation in female mice did not impact glucose homeostasis in chow-fed mice, but promoted high fat diet (HFD)-induced obesity and hyperglycemia post-exposure (22). Therefore, background level TCDD exposure alone may not induce diabetes but may increase diabetes susceptibility when challenged with a secondary metabolic stressor, such as HFD feeding. Whether this is sex-specific remains to be determined.

The effects of concurrent TCDD exposure and HFD feeding are not well understood. Studies have shown that HFD-induced hepatic fatty acid deposition is worsened following TCDD exposure in mice (23,24), which supports the hypothesis that concurrent TCDD exposure and HFD-feeding is more deleterious than either alone in hepatic tissue. However, the potential impact on systemic glucose homeostasis and the endocrine pancreas have not been reported. The purpose of this study was to determine whether prolonged exposure to a physiologically relevant dose of TCDD impairs beta cell function and/or glucose homeostasis in a sex-dependent manner in either chow-fed or HFD-fed mice.

2. Material and Methods

2.1 Animals

Male and female C57BL/6 mice, 6-8 weeks old (Charles River; Raleigh, NC, USA), were maintained on a 12-hour light/dark cycle. All mice received *ad libitum* access to a standard chow diet for 1 week prior to starting experimental treatments. All experiments were approved by Carleton University and University of Ottawa Animal Care Committees and carried out in accordance with Canadian Council on Animal Care guidelines. All experimental groups were matched for mean body weight and fasting blood glucose levels prior to starting treatments to ensure that no group was statistically different from another.

Male and female mice received intraperitoneal (i.p.) injections of corn oil (CO; vehicle control, 25 ml/kg) (#48599, Sigma Aldrich, St. Louis, MO, USA) or a low-dose of TCDD (20 ng/kg/d) (Sigma Aldrich, # 48599) 2x/week for 12 weeks (**Fig. 1A)**. Simultaneously, mice were fed either standard rodent chow (20% fat, 66% carbohydrate, 14% protein; #2918, Harlan Laboratories, Madison, WI, USA) or a HFD (45% fat, 35% carbohydrate, 20% protein; #D12451, Cedarlane, Burlington, ON, Canada), generating the following experimental groups (n=10 per group per sex): COChow, COHFD, TCDDChow, TCDDHFD. Whole pancreas was isolated from a subset of mice at week 12 of the study and stored in 4% paraformaldehyde (PFA; #AAJ19943K2, Thermo Fisher Scientific, Waltham, MA, USA) for 24-hours, followed by long-term storage in 70% ethanol for histological analysis (n=4-5 per group per sex). Pancreatic islets were isolated from a different subset of female mice at week 12 and stored in RNAlater (#76106, Qiagen, Hilden, Germany) for analysis by quantitative real-time PCR (qPCR) and TempO-Seq® (n = 3-5 per group).

2.2 Metabolic Assessments

All metabolic assessments were performed on conscious, restrained mice. Blood samples were collected via the saphenous vein using heparinized microhematocrit tubes. Blood glucose was measured using a handheld glucometer (Johnson & Johnson, New Brunswick, NJ, USA).

Body weight and blood glucose measurements were performed weekly following a 4-hour morning fast. For all metabolic assessments, time 0 indicates the blood collected prior to glucose or insulin administration. For GTTs, mice received an i.p. bolus of glucose (2 g/kg) following a 4-hour fast. Blood samples were collected at 0, 15, and 30 minutes for measuring plasma insulin levels by ELISA (#80-INSMSU-E01, ALPCO, Salem, NH, USA). For insulin tolerance tests (ITT), mice received an i.p. bolus of insulin (0.7 IU/kg, #02024233, Novo Nordisk, Toronto, Canada) following a 4-hour morning fast.

2.3 Immunofluorescence Staining and Image Quantification

Tissues were processed and embedded in paraffin wax blocks (University of Ottawa Heart Institute, Ottawa, ON, Canada) and then sectioned (5 µm). Immunofluorescence staining was performed as previously described (20). In brief, slides were deparaffinized with sequential incubations in xylene and ethanol. Heat-induced epitope retrieval was performed in 10 mM citrate buffer at 95°C for 10-15 minutes, and slides were incubated with Dako Serum Free Protein Block (#X090930-2, Agilent, Santa Clara, CA, USA) at room temperature. Slides were incubated overnight at 4°C with primary antibodies, and then for 1-hour at room temperature with secondary antibodies. Coverslips were mounted with Vectashield® hardset mounting medium with DAPI (#H-1500, Vector Laboratories, Burlingame, CA, USA).

The following primary antibodies were used: rabbit anti-insulin (1:200, C27C9, #3014, Cell Signaling Technology), and mouse anti-glucagon (1:1000; #G2654, Sigma Aldrich). The following secondary antibodies were used: goat anti-mouse IgG (H+L) secondary antibody, Alexa Fluor 488 (1:1000, Invitrogen, #A11029); and goat anti-rabbit IgG (H+L) secondary antibody, Alexa Fluor 594 (1:1000, Invitrogen, #A11037).

Whole pancreas sections were imaged using a Zeiss Axio Observer 7 microscope, and immunofluorescence was manually quantified using Zen Blue 2.6 software (Zeiss, Oberkochen, Germany). For all measurements, a range of 4-36 islets per mouse were quantified and the average was reported for each biological replicate. The % hormone$^+$ area per islet was calculated as [(hormone$^+$ area / islet area) x 100].

2.4 Islet Isolation

Islets were isolated by pancreatic duct injections with collagenase (1000 U/ml; #C7657, Sigma-Aldrich), as previously described (20). In brief, inflated pancreas tissue was excised and incubated at 37°C for 12 minutes, and the collagenase reaction quenched with cold Hank's balanced salt solution (HBSS) with 1 mM $CaCl_2$. Pancreas tissue was washed in HBSS+$CaCl_2$, resuspended in Ham's F-10 (#SH30025.01, HyClone, GE Healthcare Biosciences, Pittsburgh, PA, USA) containing 7.5% BSA (#10775835001, Sigma-Aldrich) and 1% Penicillin-Streptomycin (#30-002-CI, Corning, Tewksbury, MA, USA), and filtered through a 70 µm cell strainer (#07-201-431, Corning). Islets were handpicked under a dissecting scope to >95% purity.

2.5 Quantitative Real Time PCR

RNA was isolated from pancreatic islets using the RNeasy Micro Kit (#74004, Qiagen), as per the manufacturer's instructions, with the following amendment: 7 volumes of buffer RLT + DTT were added to the samples prior to lysing with 70% EtOH. RNA quality was assessed using a Nanodrop®. DNase treatment was performed prior to cDNA synthesis with the iScript^{TM} gDNA Clear cDNA Synthesis Kit (#1725035, Bio-Rad, Mississauga, ON, Canada). qPCR was performed using SsoAdvanced Universal SYBR Green Supermix (Bio-Rad, #1725271) and run on a CFX96 or CFX394 (Bio-Rad). *Ppia* was used as the reference gene since it displayed stable expression under control and treatment conditions. Data were analyzed using the $2^{\Delta\Delta CT}$ relative quantitation method. Primer sequences are listed in **Supp. Table 1**.

2.6 TempO-Seq®

Gene expression was measured in control and experimental whole islets (4 treatment groups; n = 3-4 per group) using the TempO-Seq® Mouse Whole Transcriptome panel in a 96-well format, according to the TempO-Seq® Assay User Guide (BioSpyder Technologies Inc, Carlsbad, CA). Briefly, 2 µl of mouse islet RNA was diluted with 2 µl of 2x TempO-Seq lysis buffer, resulting in samples ready for assay input in 1x TempO-Seq® Enhanced Lysis Buffer (RNA input range = 15.5-98 ng/µl, all within recommended limits for whole transcriptome TempO-Seq® assays). Experimental samples, in addition to a positive control (100 ng/µl of Universal Mouse Reference RNA; Agilent, cat # 750600) and a negative control (1x TempO-Seq® Enhanced Lysis Buffer alone) were hybridized to the Detector Oligo (DO) Pool in an Annealing Mix for panels with > 5,000 probes for 10 min at 70°C followed by a temperature gradient with a ramp rate of 0.5°C/min to 45°C over 50 min with a 16-hour hold at 45°C and then cooled to 25°C. Hybridization was followed by nuclease digestion to eliminate excess, unbound, or incorrectly bound DOs at 37°C for 90 min. A pool of amplification templates was then generated by ligating the DO pairs bound to adjacent target sequences for 60 min at 37°C, followed by a 15 min enzyme denaturation at 80°C. The control and experimental amplification templates (10 µl of ligated DOs) were pipetted into their respective wells of the 96-well PCR Pre-Mix and Primer plate. Amplification proceeded using a CFX96 Real-Time PCR Detection System (Bio-Rad) to incorporate a unique sample index/tag sequence and the sequencing adaptors for each sample using the following PCR settings: 37°C for 10 min, 95°C for 1 min; 25 cycles of 95°C for 10 sec, 65°C for 30 sec, 68°C for 30 sec (with optical read for visual sample QC); 68°C for 2 min; hold at 25°C prior to library pooling and purification. Library purification was achieved by pooling and purifying labelled amplicons using the NucleoSpin® Gel and PCR Clean-up kits (Takara Bio USA, Inc, Mountain View, CA USA) with three modifications to the NucleoSpin® User Manual, including the addition of a second wash with buffer NT3, an increase of the spin-to-dry step from 1 min to 10 min, and an additional elution with NE buffer to maximize the library yield. The pooled and purified library was quantified using the Universal KAPA Library Quantification kit for Illumina platforms (Roche, # KK4824). The pooled TempO-Seq® library was sequenced in-house using the NextSeq® 500/550 High Output Kits v2 (75 cycles) on an Illumina NextSeq 500 High-Throughput Sequencing System (Illumina, San Diego, CA, USA). A median read depth of 2 million reads/sample was achieved.

Reads were extracted from the BCL files, demultiplexed (i.e. assigned to respective sample files) and were processed into FASTQ files with bcl2fastq v.2.17.1.14. The FASTQ files were processed with the "pete.star.script_v3.0" supplied by BioSpyder. Briefly, the script uses star v.2.5 to align the reads and the qCount function from QuasR to extract the feature counts specified in a GTF file from the aligned reads. The data were then passed through internal quality control scripts. Boxplots of the log2 CPM (counts per million) were plotted to ensure a reproducible distribution between replicates within a group. Hierarchical clustering plots were generated (hclust function: default linkage function of hclust function in R; complete-linkage) using a distance metric defined as 1-Spearman correlation in order to identify potential outliers. Probes with low counts (i.e. less than a median of 5 counts in at least one group) were flagged as absent genes and eliminated from the dataset. Differentially expressed genes (DEG) analysis was conducted using the R software (25) on the counts using the default parameters of DESeq2 (26) with respective control and exposure groups. A shrinkage estimator was applied to the fold change estimates using the apeglm method (27) using the lfcShrink() function.

Probes reaching the threshold of an adjusted p-value < 0.05 and an absolute fold change > 1.5 (on a linear scale) were defined as DEGs and were retained for pathway analysis. Gene set analysis using KEGG pathways was conducted using DAVID (28,29). Pathways with a modified Fisher's exact p-value < 0.01 were considered enriched. Data are presented as bar graphs showing pathway fold enrichment, and secondly, as bar graphs with DEG counts for pathways that were trending (p = 0.01 - 0.1) or statistically enriched (p < 0.01). Pathways that were not trending or statistically enriched are indicated on bar graphs as not having the DEG count minimum threshold for significance.

2.7 Statistical Analysis

Statistical analysis was performed using GraphPad Prism Software (GraphPad Software Inc., La Jolla, CA). Specific statistical tests are indicated in the figure legends and $p < 0.05$ was considered statistically significant for all analyses. Statistically significant outliers were detected by a Grubbs' test with $\alpha = 0.05$. All data were tested for normality using a Shapiro-Wilk test and for equal variance using either a Brown-Forsyth test (for one-way ANOVAs) or an F test (for unpaired t tests). Non-parametric statistics were used in cases where the data failed normality or equal variance tests. Parametric tests were used for all two-way ANOVAs, but normality and equal variance were tested on area under the curve values and by one-way ANOVAs. Data in line graphs are presented as mean ± SEM. Data in box and whisker plots are displayed as median, with whiskers representing maximum and minimum values. Each individual data point represents a different biological replicate (i.e. individual mouse).

2.8 Data and Resource Availability

The datasets generated and/or analyzed during the current study are available from the corresponding author upon reasonable request. TempO-Seq® data have been submitted to National Centre for Biotechnology Information (NCBI) Gene Expression Omnibus (GEO) and are accessible under accession number GSE144765.

3. Results

3.1 Low-dose TCDD exposure does not impact body weight or fasting blood glucose levels in mice

Male and female mice were exposed to CO (vehicle) or 20 ng/kg/d TCDD 2x/week for 12 weeks, and simultaneously fed either a chow diet or 45% HFD (**Fig. 1A**). We were particularly interested in whether low-dose TCDD exposure alone would promote weight gain (i.e. COChow vs TCDDChow) and/or accelerate diet-induced obesity (i.e. COHFD vs TCDDHFD), as previously seen in female mice exposed to TCDD during pregnancy (22). Interestingly, TCDD exposure had no effect on body weight in chow-fed females in this study (**Fig. 1B**). Female mice were also resistant to HFD-induced weight gain within the 12-week study timeframe, regardless of chemical exposure (**Fig. 1B**). Likewise, TCDD exposure did not alter body weight in chow-fed or HFD-fed male mice, but HFD feeding promoted significant weight gain in male mice after 80 days (**Fig. 1C**). TCDD did not influence fasting blood glucose levels in any group, but HFD feeding caused fasting hyperglycemia in both CO- and TCDD-exposed females (**Fig. 1D,E**) and males (**Fig. 1F,G**).

3.2 TCDD exposure accelerates the onset of HFD-induced glucose intolerance in female mice

TCDD had no effect on glucose tolerance in chow-fed female or male mice at weeks 4 and 8 of the study (COChow vs TCDDChow; **Fig. 2**). However, we observed an interaction between TCDD exposure and HFD feeding in female mice (**Fig. 2A-D**). At week 4, HFD feeding had no impact on glucose tolerance in CO-exposed females (COChow vs COHFD; **Fig. 2Aii,2B**), but TCDDHFD females were significantly hyperglycemic at 15- and 30-minutes post-glucose bolus and had a significantly elevated overall glucose excursion compared to TCDDChow females (**Fig. 2Aiii,2B**). By week 8, both COHFD and TCDDHFD females were glucose intolerant compared to chow-fed females (**Fig. 2C,D**). In contrast, HFD-fed male mice were significantly hyperglycemic during the GTT after 4 and 8 weeks of exposure compared to chow-fed males, irrespective of chemical exposure (**Fig. 2E-H**). In other words, TCDD-exposed and CO-exposed males showed similar responses to HFD feeding (**Fig. 2E-H**), whereas HFD-fed female mice had accelerated onset of hyperglycemia in the presence of TCDD (**Fig. 2A-D**).

3.3 TCDD-exposed female mice lack a compensatory hyperinsulinemic response to HFD feeding but show normal insulin tolerance

After 8 weeks of HFD feeding, COHFD females showed an expected compensatory increase in plasma insulin levels during the GTT (**Fig. 3A**), with ~2.3-fold more insulin overall than COChow females (**Fig. 3A-AUC**). In contrast, plasma insulin levels in TCDDHFD females were comparable to COChow and TCDDChow females (**Fig. 3A**). TCDD did not impact insulin levels in either chow-fed or HFD-fed male mice (**Fig. 3B**), but rather diet had an overall effect on plasma insulin levels in males (**Fig. 3B**). These results suggest that TCDD exposure causes abnormal insulin secretion in HFD-fed females only.

To determine whether changes in peripheral insulin sensitivity were also contributing to the accelerated hyperglycemia in TCDDHFD females, we performed ITTs at weeks 5 and 9. HFD-fed male and female mice were not overtly insulin resistant in this study (**Fig. 3C-F**). At week 5, COHFD females were slightly more insulin sensitive than COChow females at 60 minutes after the insulin bolus (**Fig. 3C**), and at week 9 TCDDChow females were modestly more insulin sensitive at 15 minutes post-bolus compared to COChow females (**Fig. 3E**), but there were no changes in overall blood glucose levels during the ITTs (**Fig. 3C-F,AUC**).

We also measured expression of genes involved in insulin-dependent lipogenesis and gluconeogenesis pathways in the liver at week 12 as another indicator of insulin sensitivity. In females, HFD feeding significantly downregulated genes involved in gluconeogenesis (**Supp. Fig. 1A**), including *G6pc* (glucose-6-phosphatase catalytic subunit), *Ppargc1a* (peroxisome proliferator-activated receptor gamma coactivator 1 alpha), and *Pck1* (phosphoenolpyruvate carboxykinase 1). There was a significant interaction between TCDD and HFD exposure on expression of *Acacb* (acetyl-CoA carboxylase beta; **Supp. Fig. 1A**), but this was modest and unlikely to explain the differences observed in plasma insulin levels or glucose homeostasis in female mice. There were no differences in any of the measured genes in the liver of male mice following TCDD and/or HFD exposure (**Supp. Fig. 1B**).

3.4 Islet size and endocrine composition were unchanged by TCDD exposure

To investigate why TCDD-exposed female mice did not develop hyperinsulinemia following HFD feeding, we examined islet size and endocrine cell composition in the pancreas at week 12. We predicted that HFD-fed mice might show increased islet size compared to chow-fed mice, but this

was not the case in either sex (**Fig. 4A,D,G**). Surprisingly, there was a significant overall effect of TCDD exposure to increase average islet size in male mice (**Fig. 4D**, $p_{chemical} < 0.05$). The percentage of islet area that was immunoreactive for either insulin (**Fig. 4B,E,G**) or glucagon (**Fig. 4C,F,G**) was unchanged in either sex.

3.5 TCDDHFD female mice have enriched endocrine-related pathways in islets relative to COChow females

Since our histological findings did not explain the phenotype observed in TCDDHFD females, we performed TempO-Seq® analysis on isolated islets from a subset of females at week 12 of the study to assess whole transcriptomic changes. We analyzed our TempO-Seq® results using 3 approaches. First, we compared TCDD-exposed females to their respective CO-exposed control (TCDDChow vs COChow and TCDDHFD vs COHFD) (**Supp. Fig. 3**), we then compared all experimental groups to COChow (**Fig. 5, 6**), and lastly we compared HFD-fed females to their respective chow-fed control (COHFD vs COChow and TCDDHFD vs TCDDChow) (**Fig. 7, 8**).

We compared TCDD-exposed females to CO-exposed females to assess the effect of TCDD exposure on chow or HFD diet. We observed 595 unique DEGs in TCDDChow females, and only 121 unique DEGs in TCDDHFD females compared to their respective CO-exposed control (**Supp. Fig. 3A**). Surprisingly, KEGG pathway analysis did not reveal any significant pathway alterations in TCDDHFD females when compared to COHFD females (refer to **Fig. 5Bi** for TCDDChow vs COChow pathway analysis). However, we did find that *Slc2a2* and *G6pc2*, two genes essential for proper beta cell function, were the most downregulated genes in TCDDHFD females compared to COHFD females (**Supp. Fig. 3B**). These findings prompted us to assess our TempO-Seq® data using a different approach to better understand TCDD-induced changes in the islet transcriptome.

We next compared all experimental groups to COChow females to investigate the effect of TCDD or HFD feeding alone (i.e. TCDDChow and COHFD, respectively), and in combination (TCDDHFD), to determine whether there is an interactive effect of HFD feeding and TCDD. TCDDChow females had 607 DEGs, whereas COHFD females had 2,121 DEGs and TCDDHFD females had 2,667 DEGs compared to COChow females (**Fig. 5A**). Interestingly, only 33 DEGs were unique to TCDD-exposed groups (i.e. TCDDChow and TCDDHFD) and unchanged in COHFD females. In addition, only 79 genes were uniquely changed in TCDDChow females (**Fig. 5A**). These results suggest that TCDD alone has relatively minor effects on gene expression in whole islets, which supports our *in vivo* observations (**Figs. 1-4**). In contrast, 1060 genes were altered in both HFD groups but not in the TCDDChow condition; 1,197 DEGs were unique to TCDDHFD females and 566 DEGs unique to COHFD females (**Fig. 5A**), suggesting that TCDD may be driving abnormal changes in gene expression in response to HFD feeding.

We performed KEGG pathway analysis on all DEGs for each experimental group compared to COChow, as shown in **Fig. 5A** (i.e. TCDDChow- 607 DEGs; COHFD- 2,121 DEGs; TCDDHFD- 2,667 DEGs). Since pathway enrichment is determined based on total number of DEGs and the number of DEGs varied between our experimental groups (**Fig. 5A**), we presented pathway analysis as both pathway fold enrichment and number of DEGs within each pathway to avoid misinterpretation. We first assessed pathways that were uniquely enriched in TCDDChow females to determine the effects of TCDD alone on the islet transcriptome (**Fig. 5Bi**). As expected, "Xenobiotic Metabolism by CYP450" was highly enriched in TCDDChow compared to COChow

females, and 50% of the pathways enriched in TCDDChow females were involved in drug/chemical exposure, suggesting that TCDD alone mainly alters drug metabolism in islets. It is important to note that although "Xenobiotic Metabolism by CYP450" was not significantly enriched in COHFD or TCDDHFD females, a greater number of genes in the pathway were altered in HFD-fed than chow-fed females (**Fig. 5Bi**), suggesting that both TCDD exposure and HFD feeding alter this pathway.

We also assessed enriched pathways in COHFD and TCDDHFD females compared to COChow controls to identify transcriptomic differences that may explain why TCDDHFD females lacked a compensatory increase in insulin secretion (**Fig. 3A**). "Maturity Onset Diabetes of the Young" (MODY) was the most enriched pathway in COHFD compared to COChow females, but the number of DEGs was similar in both HFD groups irrespective of chemical treatment (**Fig. 5Bii**). In addition, "Insulin Secretion" was enriched in both HFD groups, although more genes were altered in TCDDHFD females compared to COHFD females (**Fig. 5Biv**). Interestingly, several pathways involved in beta cell function were differentially enriched in COHFD and TCDDHFD females. First, "Regulation of Actin Cytoskeleton" was significantly altered in COHFD females but not TCDDHFD females, with 35 DEGs in COHFD females (**Fig. 5Bii**). Therefore, changes in the actin cytoskeleton in islets may be a normal response to HFD feeding that is absent in the TCDDHFD condition. Second, "Circadian Rhythm" was the most enriched pathway in TCDDHFD compared to COChow females, and more genes within this pathway were changed in TCDDHFD females compared to COHFD females (**Fig. 5Bv**). Likewise, "FoxO1 Signaling Pathway" was enriched in TCDDHFD females, and more genes were altered in this pathway in TCDDHFD females compared to COHFD females (**Fig. 5Bv**). Lastly, "Thyroid Hormone Signaling Pathway" was significantly altered in TCDDHFD females only (**Fig. 5Bv**).

3.6 TCDDHFD females have inappropriate Cyp1a1 and circadian rhythm gene expression

To better understand the effect of TCDD on the islet transcriptome, we used hierarchical clustering and heatmaps organized by experimental group (**Fig. 6**, **Supp. Fig. 2**) to examine pathways of interest that were enriched in TCDDChow and TCDDHFD females compared to COChow controls (**Fig. 5**). We were particularly interested in the "Xenobiotic Metabolism by CYP450" pathway since we have previously shown that TCDD induces CYP1A1 enzymes in islets (20,21). We expected to see a clear branching structure separating CO- and TCDD-exposed females, but instead we observed a main branch that separated COChow females from all experimental groups, with overall gene expression being downregulated in all groups compared to COChow (**Fig. 6A, Supp. Fig. 2A**). However, within the main branch, TCDDChow females formed a sub-cluster, indicating slight differences in gene expression compared to HFD-fed females (**Fig. 6A**). Next, we specifically examined *Cyp1a1* expression as a marker of AhR activation by dioxin exposure (20,21) and found *Cyp1a1* was upregulated ~3.5-fold and ~3.2-fold in TCDDChow and COHFD females, respectively, compared to COChow females (**Fig. 6C**). In contrast, TCDDHFD islets showed a non-significant trend towards having only ~2-fold higher *Cyp1a1* expression compared to COChow females, and *Cyp1a1* levels remained significantly lower than in TCDDChow females (**Fig. 6C**). These results suggest that crosstalk between TCDD exposure and HFD feeding prevents normal *Cyp1a1* induction in islets. These findings were validated by qPCR (**Fig. 6D**).

We also assessed circadian rhythm gene expression patterns since this pathway was the most enriched in TCDDHFD females (**Fig. 5v**). Unlike other pathways analysed in this study, the

hierarchical heatmap for "Circadian Rhythm" was unclear (**Supp. Fig 2B**). We observed two main branches in the hierarchical heatmap. The right branch clustered based on diet with HFD mice separated from chow mice, and showed further grouping within the diet subclusters that was driven by chemical exposure (**Supp. Fig 2B**). However, the left branch of the hierarchal plot comprised all experimental groups and showed no clear pattern of clustering, preventing us from conclusively identifying overall changes in circadian rhythm (**Supp. Fig 2B**). Instead, we used a heatmap organized by experimental group to assess changes in expression of individual circadian rhythm genes (**Fig. 6B**). Interestingly, key regulators of circadian rhythm were uniquely changed in TCDDHFD islets. For example, *Clock* was significantly upregulated in TCDDHFD islets compared to COChow islets (**Fig. 6B**,**E**). In addition, *Rorα* (retinoic acid receptor-related orphan receptor alpha), a member of the core clock machinery and a regulator of lipid/glucose homeostasis (30), was upregulated in TCDDHFD females compared to all other experimental groups (**Fig. 6B**,**F**). Lastly, *Rorγ*, another regulator of the circadian clock (30), was downregulated in TCDDHFD females compared to chow-fed females (**Fig. 6B**,**G**). Taken together, these results suggest that TCDD exposure alters circadian rhythm in islets from HFD-fed mice.

3.7 TCDD exposure promotes HFD-induced changes in amino acid metabolism genes in islets

Our *in vivo* results (**Figs. 2-3**) and previous findings from a separate study in pregnant mice (22) suggest that background exposure to TCDD accelerates HFD-induced changes in metabolism in female mice. As such, we next investigated the effects of HFD feeding on the islet transcriptome of females with either CO or TCDD background exposure (i.e. COHFD vs COChow and TCDDHFD vs TCDDChow). Interestingly, COHFD females had 1674 unique DEGs relative to COChow, whereas TCDDHFD females had 706 unique DEGs relative to TCDDChow (**Fig. 7A**), indicating that the effect of HFD feeding varies with chemical exposure. Indeed, KEGG pathway analysis revealed significant differences between COHFD and TCDDHFD females when compared to their respective chow-fed controls (**Fig. 7B**). As with our findings in **Fig. 5B**, MODY was the most enriched pathway in COHFD females; this pathway was also altered in TCDDHFD females, but to a lesser extent (**Fig. 7Bi**). "Regulation of Actin Cytoskeleton" and "PI3K-Akt Signaling Pathway" were only altered by HFD feeding when mice were on a CO background (**Fig. 7Bi**), suggesting that TCDD exposure prevents these normal responses to HFD feeding. Most interestingly, the top two most enriched pathways in TCDDHFD compared to TCDDChow females were "Alanine, Aspartate & Glutamate metabolism", and "Tyrosine Metabolism" (**Fig. 7Bii**). In fact, 40% of significantly enriched pathways in TCDDHFD females are involved in amino acid metabolism (**Fig. 7Bii**), suggesting that background exposure to TCDD promotes abnormal changes to amino acid metabolism in HFD-fed females.

3.8 TCDD promotes HFD-induced changes in MODY and alanine, aspartate, and glutamate metabolism gene expression

We generated heatmaps of the most enriched pathway in COHFD and TCDDHFD females with respect to their chow-fed controls (pathway enrichment shown in **Fig. 7B**). Interestingly, the "MODY" heatmap showed that TCDDHFD females form a unique cluster and generally had lower gene expression compared to all other groups (**Fig. 8A, Supp. Fig. 2C**), suggesting an interactive effect of HFD feeding and TCDD exposure on expression of islet-specific genes. Furthermore, we noticed a distinct pattern in genes essential for maintaining beta cell function (**Fig. 8A, 8C-H, Supp. Fig. 2C**). *MafA* and *Slc2a2* were significantly downregulated in TCDDHFD females compared to COChow and TCDDChow females, whereas expression was only trending towards

being downregulated in COHFD females (**Fig. 8C,H**). *MafA* results were validated by qPCR (**Fig. 8D**). Similarly, *Hnf4a* was downregulated by HFD feeding, but this effect was worsened in TCDD-exposed females (**Fig. 8G**), whereas *Pax6* was only downregulated in TCDDHFD females compared to COChow females (**Fig. 8F**). Interestingly, *Nkx6.1* was upregulated in COHFD compared to COChow females, but expression was downregulated in TCDDHFD females compared to both COHFD and TCDDChow females (**Fig. 8E**). These results suggest that TCDD exposure alters diet-induced changes in beta cell specific genes.

The "Alanine, Aspartate and Glutamate Metabolism" pathway heatmap showed that COHFD and TCDD-exposed females formed a separate cluster compared to COChow females, suggesting that both HFD feeding and TCDD exposure alter amino acid metabolism (**Fig. 8B, Supp. Fig. 2D**). Interestingly, TCDDHFD females formed a separate subcluster compared to both TCDDChow and COHFD females, suggesting that TCDD alters HFD-induced changes in amino acid metabolism (**Fig. 8B**).

4. Discussion

Our study demonstrates that the effects of physiologically relevant low-dose TCDD exposure on glucose metabolism are sex-dependent. In this 12-week study, low-dose TCDD exposure accelerated the onset of HFD-induced hyperglycemia in female, but not male, mice by at least 4 weeks. Furthermore, HFD feeding induced hyperinsulinemia in CO-exposed female mice and both TCDD- and CO-exposed male mice, but failed to induce compensatory hyperinsulinemia in TCDD-exposed females. These findings are in line with our previous work showing that female mice exposed to low-dose TCDD during pregnancy/lactation and subsequently fed HFD later in life had accelerated onset of hyperglycemia and transient low glucose-induced plasma insulin levels compared to COHFD females (22). Furthermore, RNA-Seq analysis on isolated islets revealed that TCDD exposure promoted abnormal changes to endocrine and metabolic pathways in HFD-fed females. TCDD exposure alone did not impact glucose homeostasis or plasma insulin levels in either sex in this study or in the pregnancy model (22), suggesting that this persistent pollutant is more of a concern when combined with a secondary metabolic stressor.

There were no differences in islet size or pancreatic endocrine cell composition to explain the lack of diet-induced hyperinsulinemia in TCDDHFD females. However, our TempO-Seq® analysis suggests a defect in beta cell function and impaired metabolic adaptability. For example, expression of MODY genes differed between TCDDHFD and COHFD females, indicating an interaction between TCDD and HFD on beta cell specific genes. In fact, the diet-induced decrease in *MafA*, *Hnf4α*, and *Slc2a2* was worsened in TCDD-exposed females, whereas *Pax6* was downregulated only in TCDDHFD compared to COChow females. Further, the compensatory increase in *Nkx6.1* in COHFD females compared to COChow was absent in TCDDHFD females. These findings are consistent with our pregnancy model showing a reduced proportion of beta cells expressing MAFA in the pancreas of TCDDHFD females compared to COHFD females (22). The beta cell transcription factors MAFA, PDX1, HNF4α, and PAX6 form an essential network for maintaining beta cell identity and regulating genes involved in insulin secretion (e.g. *Slc2a2*); inactivation of these genes is associated with beta cell dedifferentiation and metabolic inflexibility (31). Under conditions of nutrient overload, beta cells must compensate for changes in metabolic

demand by altering the rate and amount of insulin secreted; failure to adapt is associated with diabetes (32). Our results suggest that low-dose TCDD exposure promotes diet-induced beta cell dedifferentiation, which could contribute to impaired metabolic adaptability and increase diabetes risk in female mice. Further research is required to support this hypothesis.

TempO-Seq® analysis also revealed unique changes in metabolic and endocrine pathways in TCDDHFD females compared to chow-fed females that further support a defect in metabolic adaptability. We focus on two pathways of interest here; however, future studies should further investigate the interactive effect of TCDD and HFD on other pathways that were enriched in our study, including "Thyroid Signalling", "Foxo1 Signaling", and "Regulation of Actin Cytoskeleton". Our analysis revealed changes in the "Circadian Rhythm" pathway in islets from TCDDHFD females. Although hierarchal clustering did not reveal clear overall patterns of gene expression, TCDD impairs normal alterations in key islet circadian rhythm genes during HFD feeding. These data are interesting given that alterations to the circadian clock have been associated with diabetes, obesity, and metabolic syndrome in humans (33–35). Abnormal expression of clock genes has also been reported in islets from type 2 diabetic donors compared to non-diabetic donors, and insulin content was positively correlated with expression of clock genes, suggesting that disruptions to the islet circadian clock contributes to beta cell dysfunction and diabetes pathogenesis (36,37). In fact, knockdown of *Clock* in human islets led to dysfunctional glucose-stimulated insulin secretion and altered the expression of genes involved in insulin secretion (38). Islet-specific *Clock* knockout mice also exhibit hypoinsulinemia, hyperglycemia, glucose intolerance, and an impaired insulin secretory response (39). Lastly, experimental disruption of circadian rhythms accelerates the onset of hyperglycemia and loss of functional beta cells in diabetes-prone rats (40). Therefore, it is possible that the glucose intolerance and reduced plasma insulin levels in TCDDHFD female mice involves altered islet circadian rhythms, but more detailed analysis is required to understand the mechanism(s) involved.

Prolonged low-dose TCDD exposure promoted alterations to amino acid metabolism pathways in HFD-fed females. TCDD exposure has previously been associated with changes to circulating amino acid concentrations (41–43) and hepatic amino acid metabolism genes *in vivo* (44) and *in vitro* (45,46). Our data indicate that TCDD may also alter amino acid metabolism in islets under conditions of HFD feeding, which may have important implications for diabetes risk. Amino acids play an important role in maintaining beta cell function (47). Several studies have shown that amino acids enhance glucose-stimulated insulin secretion (48–50), and may indirectly regulate lipid-stimulated insulin secretion by activating enzymes involved in lipid metabolism (51,52). Amino acids also promote the expression of genes involved in beta cell signal transduction, metabolism, and insulin secretion (e.g. *Pdx1*) (53,54). Moreover, perturbations to amino acid metabolism have been associated with type 2 diabetes, obesity, and insulin resistance (55). Our data suggest that impaired amino acid metabolism in islets contributes to the reduced plasma insulin levels and hyperglycemia observed in TCDDHFD female mice, but further investigation is required.

Lastly, our TempO-Seq® analysis revealed interesting changes in "Xenobiotic Metabolism by CYP450". We have previously shown that single high-dose and multiple low-dose TCDD exposure induced CYP1A1 gene expression and enzyme activity in islets from male mice (20,21). The present study demonstrates that *Cyp1a1* is also upregulated in female islets following low-

dose TCDD exposure. We also found that HFD feeding induces *Cyp1a1* expression in islets to a similar degree as TCDD exposure, suggesting a role for CYP1A1 enzymes in islets beyond xenobiotic metabolism. Interestingly, we have previously shown that male *Cyp1a1/1a2* knockout mice had suppressed glucose-stimulated insulin secretion compared to wildtype controls, pointing to a non-conventional role of CYP enzymes in maintaining beta cell function (20). In this study, the TCDD- and HFD-induced increase in *Cyp1a1* was suppressed in TCDDHFD females, suggesting cross-talk between TCDD and HFD feeding. We previously observed that TCDD exposure upregulated *CYP1A1* ~26-fold in human islets, but this induction was completely prevented by cotreatment with cytokines (20). Given that HFD feeding increases cytokine signalling (56), we speculate that there may be an interaction between AhR and cytokine signalling pathways in this mouse model. Whether impaired *Cyp1a1* induction contributes to the metabolic phenotype observed in TCDDHFD females remains unclear.

To our knowledge this is the first study to do a head-to-head comparison of the effects of physiologically relevant low-dose TCDD exposure on diabetes risk in male and female mice. Our findings are consistent with epidemiological evidence showing that females with high serum pollutant levels have a higher risk of developing diabetes than males. However, few epidemiological studies have examined sex-differences in the general population with background level of pollutant exposure, and most do not consider diet as a confounding variable when studying the association between pollutant exposure and diabetes risk. Our mouse study shows that 12 weeks of low-dose TCDD alone does not cause diabetes but does increase susceptibility to diet-induced diabetes in female mice, emphasizing the need to study the interaction of pollutants with other metabolic stressors such as diet.

Acknowledgements
We thank Salar Farokhi Boroujeni and Andrea Rowan-Carroll for their technical assistance with sample analysis for this project. This research was supported by a Canadian Institutes of Health Research (CIHR) Project Grant (#PJT-2018-159590), Natural Sciences and Engineering Research Council of Canada (NSERC) Discovery Grant (RGPIN-2017-06272), the Canada Foundation for Innovation John R. Evans Leaders Fund (#37231), and an Ontario Research Fund award. M.P.H. was supported by an Ontario Graduate Scholarship (OGS) and CIHR CGS-D award. H.B. received a NSERC Undergraduate Student Research Award (USRA) and a Carleton University Walker Summer Research Award. J.E.B. is the guarantor for this work.

Author Contributions

J.E.B. and G.M. conceived the experimental design. J.E.B., G.M., and M.P.H. wrote the manuscript. G.M., M.P.H., H.L.B., J.Z., S.F.B, K.R.C.R., A.W., R.G., J.K.B., C.L.Y., and J.E.B. were involved with acquisition, analysis, and interpretation of data. All authors contributed to manuscript revisions and approved the final version of the article.

Declaration of Interest

The authors declare no competing interests.

References

1. **Saeedi P, Petersohn I, Salpea P, Malanda B, Karuranga S, Unwin N, Colagiuri S, Guariguata L, Motala AA, Ogurtsova K, Shaw JE, Bright D, Williams R.** Global and regional diabetes prevalence estimates for 2019 and projections for 2030 and 2045: results from the International Diabetes Federation Diabetes Atlas, 9th edition. *Diabetes Res. Clin. Pract.* 2019;157:107843.
2. **Wu Y, Ding Y, Tanaka Y, Zhang W.** Risk factors contributing to type 2 diabetes and recent advances in the treatment and prevention. *Int. J. Med. Sci.* 2014;11(11):1185–1200.
3. **Taylor KW, Novak RF, Anderson HA, Birnbaum LS, Blystone C, Devito M, Jacobs D, Köhrle J, Lee DH, Rylander L, Rignell-Hydbom A, Tornero-Velez R, Turyk ME, Boyles AL, Thayer KA, Lind L.** Evaluation of the association between persistent organic pollutants (POPs) and diabetes in epidemiological studies: a national toxicology program workshop review. *Environ. Heal. Perspect.* 2013;121(7):774–783.
4. **Sun W, Clark JM, Park Y.** Environmental pollutants and type 2 diabetes: a review of human studies. *Toxicol. Environemtnal Chem.* 2017;99(9–10):1283–1303.
5. **Kuo CC, Moon K, Thayer KA, Navas-Acien A.** Environmental chemicals and type 2 diabetes: An updated systematic review of the epidemiologic evidence. *Curr. Diab. Rep.* 2013;13(6):831–849.
6. **Lee DH, Lee IK, Song K, Steffes M, Toscano W, Baker BA, Jacobs DR.** A strong dose-response relation between serum concentrations of persistent organic pollutants and diabetes: results from the National Health and Examination Survey 1999-2002. *Diabetes Care* 2006;29:1638–1644.
7. **Lee YM, Ha CM, Kim SA, Thoudam T, Yoon YR, Kim DJ, Kim HC, Moon HB, Park S, Lee IK, Lee DH.** Low-dose persistent organic pollutants impair insulin secretory function of pancreatic b-cells: human and in vitro evidence. *Diabetes* 2017;66(10):2669–2680.
8. **Wang SL, Tsai PC, Yang CY, Guo YL.** Increased risk of diabetes and polychlorinated biphenyls and dioxins: a 24-year follow-up study of the Yucheng cohort. *Diabetes Care* 2008;31(8):1574–1579.
9. **Lee DH, Lee INK, Jin SH, Steffes M, Jacobs DR.** Association between serum concentrations of persistent organic pollutants and insulin resistance among nondiabetic adults: Results from the National Health and Nutrition Examination Survey 1999-2002. *Diabetes Care* 2007;30(3):622–628.
10. **Roh E, Kwak SH, Jung HS, Cho YM, Pak YK, Park KS, Kim SY, Lee HK.** Serum aryl hydrocarbon receptor ligand activity is associated with insulin resistance and resulting type 2 diabetes. *Acta Diabetol.* 2015;52(3):489–495.
11. **Rylander L, Rignell-Hydbom A, Hagmar L.** A cross-sectional study of the association between persistent organochlorine pollutants and diabetes. *Environ. Heal. A Glob. Access Sci. Source* 2005;4:28.
12. **Airaksinen R, Rantakokko P, Eriksson JG, Blomstedt P, Kajantie E, Kiviranta H.** Association between type 2 diabetes and exposure to persistent organic pollutants. *Diabetes Care* 2011;34(9):1972–2303.
13. **Glynn AW, Granath F, Aune M, Atuma S, Darnerud PO, Bjerselius R, Vainio H, Weiderpass E.** Organochlorines in Swedish women: determinants of serum concentrations. *Environ. Health Perspect.* 2003;111:349–355.

14. **Michalek JE, Pavuk M.** Diabetes and cancer in veterans of operation Ranch Hand after adjustment for calendar period, days of spraying, and time spent in Southeast Asia. *J. Occup. Environ. Med.* 2008;50(3):330–340.
15. **Consonni D, Pesatori AC, Zocchetti C, Sindaco R, D'Oro LC, Rubagotti M, Bertazzi PA.** Mortality in a population exposed to dioxin after the Seveso, Italy, accident in 1976: 25 years of follow-up. *Am. J. Epidemiol.* 2008;167(7):847–858.
16. **Vena J, Boffetta P, Becher H, Benn T, Bas Bueno-de-Mesquita H, Coggon D, Colin D, Flesch-Janys D, Green L, Kauppinen T, Littorin M, Lynge E, Mathews JD, Neuberger M, Pearce N, Pesatori AC, Saracci R, Steenland K, Kogevinas M.** Exposure to dioxin and nonneoplastic mortality in the expanded IARC international cohort study of phenoxy herbicide and chlorophenol production workers and sprayers. *Environ. Health Perspect.* 1998;106:645–653.
17. **Pesatori AC, Zocchetti C, Guercilena S, Consonni D, Turrini D, Bertazzi PA.** Dioxin exposure and non-malignant health effects: a mortality study. *Occup. Environ. Med.* 1998;55:126–131.
18. **Vasiliu O, Cameron L, Gardiner J, DeGuire P, Karmaus W.** Polybrominated biphenyls, polychlorinated biphenyls, body weight, and incidence of adult-onset diabetes mellitus. *Epidemiology* 2006;17:352–359.
19. **WHO (World Health Organization).** *A review of human carcinogens. Part F: chemical agents and related occupations / IARC working group on the evaluation of carcinogenic risks to humans*.; 2012.
20. **Ibrahim M, MacFarlane EM, Matteo G, Hoyeck MP, Rick KRC, Boroujeni SF, Copley C, O'Dwyer S, Bruin JB.** Functional cytochrome P450 1a enzymes are induced in mouse and human islets following pollutant exposure. *Diabetologia* 2020;63:162–178.
21. **Hoyeck MP, Blair H, Ibrahim M, Solanki S, Elsawy M, Prakash A, Rick KRC, Matteo G, O'Dwyer S, Bruin JB.** Long-term metabolic consequences of acute dioxin exposure differ between male and female mice. *Sci. Rep.* 2020;10(1):1448.
22. **Hoyeck MP, Merhi R, Blair H, Spencer CD, Payant MA, Martin Alfonso DI, Zhang M, Matteo G, Chee MJ, Bruin JB.** Female mice exposed to low-doses of dioxin during pregnancy and lactation have increased susceptibility to diet-induced obesity and diabetes. *Mol. Metab.* 2020;101104. doi:10.1016/j.molmet.2020.101104.
23. **Angrish MM, Mets BD, Jones AD, Zacharewski TR.** Dietary fat is a lipid source in 2,3,7,8-Tetrachlorodibenzo-ρ-Dioxin (TCDD)-elicited hepatic steatosis in C57BL/6 mice. *Toxicol. Sci.* 2012;128(2):377–386.
24. **Duval C, Teixeira-Clerc F, Leblanc AF, Touch S, Emond C, Guerre-Millo M, Lotersztajn S, Barouki R, Aggerbeck M, Coumoul X.** Chronic exposure to low doses of dioxin promotes liver fibrosis development in the C57BL/6J diet-induced obesity mouse model. *Environ. Health Perspect.* 2017;125(3):428–436.
25. **R Core Team.** R: A language and environment for statistical computing. *R Found. Stat. Comput. Vienna, Austria* 2020. Available at: https://www.r-project.org/.
26. **Love MI, Huber W, Anders S.** Moderated estimation of fold change and dispersion for RNA-seq data with DESeq2. *Genome Biol.* 2014;15(550). doi:10.1186/s13059-014-0550-8.
27. **Zhu A, Ibrahim JG, Love MI.** Heavy-Tailed prior distributions for sequence count data: Removing the noise and preserving large differences. *Bioinformatics* 2019;35(12):2084–2092.

28. **Huang DW, Sherman BT, Lempicki RA.** Bioinformatics enrichment tools: Paths toward the comprehensive functional analysis of large gene lists. *Nucleic Acids Res.* 2009;37(1):1–13.
29. **Huang DW, Sherman BT, Lempicki RA.** Systematic and integrative analysis of large gene lists using DAVID bioinformatics resources. *Nat. Protoc.* 2009;4(1):44–57.
30. **Solt LA, Kojetin DJ, Burris TP.** The REV-ERBs and RORs: molecular links between circadian rhythms and lipid homeostasis. *Future Med. Chem.* 2011;3(5):623–638.
31. **Bensellam M, Jonas JC, Laybutt DR.** Mechanisms of β-cell dedifferentiation in diabetes: Recent findings and future research directions. *J. Endocrinol.* 2018;236(2):R109–R143.
32. **Wortham M, Sander M.** Mechanisms of β-cell functional adaptation to changes in workload. *Diabetes, Obes. Metab.* 2016;18:78–86.
33. **Barbadoro P, Santarelli L, Croce N, Bracci M, Vincitorio D, Prospero E, Minelli A.** Rotating shift-work as an independent risk factor for overweight Italian workers: a cross-sectional study. *PLoS One* 2013;8(5):e63289.
34. **Scheer FAJL, Hilton MF, Mantzoros CS, Shea SA.** Adverse metabolic and cardiovascular consequences of circadian misalignment. *Proc. Natl. Acad. Sci. U. S. A.* 2009;106(11):4453–4458.
35. **Karlsson B, Knutsson A, Lindahl B.** Is there an association between shift work and having a metabolic syndrome? Results from a population based study of 27 485 people. *Occup. Environ. Med.* 2001;58(11):747–752.
36. **Stamenkovic JA, Olsson AH, Nagorny CL, Malmgren S, Dekker-Nitert M, Ling C, Mulder H.** Regulation of core clock genes in human islets. *Metabolism.* 2012;61(7):978–985.
37. **Taneera J, Mohammed AK, Dhaiban S, Hamad M, Prasad RB, Sulaiman N, Salehi A.** RORB and RORC associate with human islet dysfunction and inhibit insulin secretion in INS-1 cells. *Islets* 2019;11(1):10–20.
38. **Saini C, Petrenko V, Pulimeno P, Giovannoni L, Berney T, Hebrok M, Howald C, Dermitzakis ET, Dibner C.** A functional circadian clock is required for proper insulin secretion by human pancreatic islet cells. *Diabetes, Obes. Metab.* 2016;18(4):355–365.
39. **Marcheva B, Ramsey KM, Buhr ED, Kobayashi Y, Su H, Ko CH, Ivanova G, Omura C, Mo S, Vitaterna MH, Lopez JP, Philipson LH, Bradfield CA, Crosby SD, Jebailey L, Wang X, Takahashi JS, Bass J.** Disruption of the clock components CLOCK and BMAL1 leads to hypoinsulinaemia and diabetes. *Nature* 2010;466:627–631.
40. **Gale JE, Cox HI, Qian J, Block GD, Colwell CS, Matveyenko A V.** Disruption of circadian rhythms accelerates development of diabetes through pancreatic beta-cell loss and dysfunction. *J. Biol. Rhythms* 2011;26(5):423–433.
41. **Christian BJ, Menahan LA, Peterson RE.** Intermediary metabolism of the mature rat following 2,3,7,8-tetrachlorodibenzo-p-dioxin treatment. *Toxicol. Appl. Pharmacol.* 1986;83(2):360–378.
42. **Unkila M, Pohjanvirta R, Macdonald E, Tuomisto JT, Tuomisto J.** Dose response and time course of alterations in tryptophan metabolism by 2,3,7,8-tetrachlorodibenzo-p-dioxin (TCDD) in the most TCDD-susceptible and the most TCDD-resistant rat strain: relationship with TCDD lethality. *Toxicol. Appl. Pharmacol.* 1994;128(2):280–292.
43. **Viluksela M, Unkila M, Pohjanvirta R, Tuomisto JT, Stahl BU, Rozman KK, Tuomisto J.** Effects of 2,3,7,8-tetrachlorodibenzo-p-dioxin (TCDD) on liver

phosphoenolpyruvate carboxykinase (PEPCK) activity, glucose homeostasis and plasma amino acid concentrations in the most TCDD-susceptible and the most TCDD-resistant rat strains. *Arch. Toxicol.* 1999;73:323–336.

44. **Boverhof DR, Burgoon LD, Tashiro C, Sharratt B, Chittim B, Harkema JR, Mendrick DL, Zacharewski TR.** Comparative toxicogenomic analysis of the hepatotoxic effects of TCDD in Sprague Dawley rats and C57BL/6 mice. *Toxicol. Sci.* 2006;94(2):398–416.
45. **Jennen D, Ruiz-Aracama A, Magkoufopoulou C, Peijnenburg A, Lommen A, van Delft J, Kleinjans J.** Integrating transcriptomics and metabonomics to unravel modes-of-action of 2,3,7,8-tetrachlorodibenzo-p-dioxin (TCDD) in HepG2 cells. *BMC Syst. Biol.* 2011;5(1):139.
46. **Jennen DGJ, Magkoufopoulou C, Ketelslegers HB, van Herwijnen MHM, Kleinjans JCS, van Delft JHM.** Comparison of HepG2 and HepaRG by whole-genome gene expression analysis for the purpose of chemical hazard identification. *Toxicol. Sci.* 2010;115(1):66–79.
47. **Newsholme P, Brennan L, Bender K.** Amino acid metabolism, β-cell function, and diabetes. *Diabetes* 2006;55:S39–S49.
48. **Smith PA, Sakura H, Coles B, Gummerson N, Proks P, Ashcroft FM.** Electrogenic arginine transport mediates stimulus-secretion coupling in mouse pancreatic β-cells. *J. Physiol.* 1997;499(3):625–635.
49. **Brennan L, Shine A, Hewage C, Paul G Malthouse J, Brindle KM, McClenaghan N, Flatt PR, Newsholme P.** A nuclear magnetic resonance-based demonstration of substantial oxidative L-alanine metabolism and L-alanine-enhanced glucose metabolism in a clonal pancreatic β-cell line: Metabolism of L-alanine is important to the regulation of insulin secretion. *Diabetes* 2002;51(6):1714–1721.
50. **Dixon G, Nolan J, McClenaghan N, Flatt PR, Newsholme P.** A comparative study of amino acid consumption by rat islet cells and the clonal beta-cell line BRIN-BD11 - The functional significance of L-alanine. *J. Endocrinol.* 2003;178(3):447–454.
51. **Gaussin V, Hue L, Stalmans W, Bollen M.** Activation of hepatic acetyl-CoA carboxylase by glutamate and Mg2+ is mediated by protein phosphatase-2A. *Biochem. J.* 1996;316:217–224.
52. **Kowluru A, Chen HQ, Modrick LM, Stefanelli C.** Activation of acetyl-coa carboxylase by a glutamate-and magnesium-sensitive protein phosphatase in the islet β-Cell. *Diabetes* 2001;50(7):1580–1587.
53. **Cunningham GA, McClenaghan NH, Flatt PR, Newsholme P.** L-alanine induces changes in metabolic and signal transduction gene expression in a clonal rat pancreatic β-cell line and protects from pro-inflammatory cytokine-induced apoptosis. *Clin. Sci.* 2005;109(5):447–455.
54. **Corless M, Kiely A, McClenaghan NH, Flatt PR, Newsholme P.** Glutamine regulates expression of key transcription factor, signal transduction, metabolic gene, and protein expression in a clonal pancreatic β-cell line. *J. Endocrinol.* 2006;190(3):719–727.
55. **Adams SH.** Emerging perspectives on essential amino acid metabolism in obesity and the insulin-resistant state. *Adv. Nutr.* 2011;2(6):445–456.
56. **Duan Y, Zeng L, Zheng C, Song B, Li F, Kong X, Xu K.** Inflammatory links between high fat diets and diseases. *Front. Immunol.* 2018;9:2649.

Figure Legends

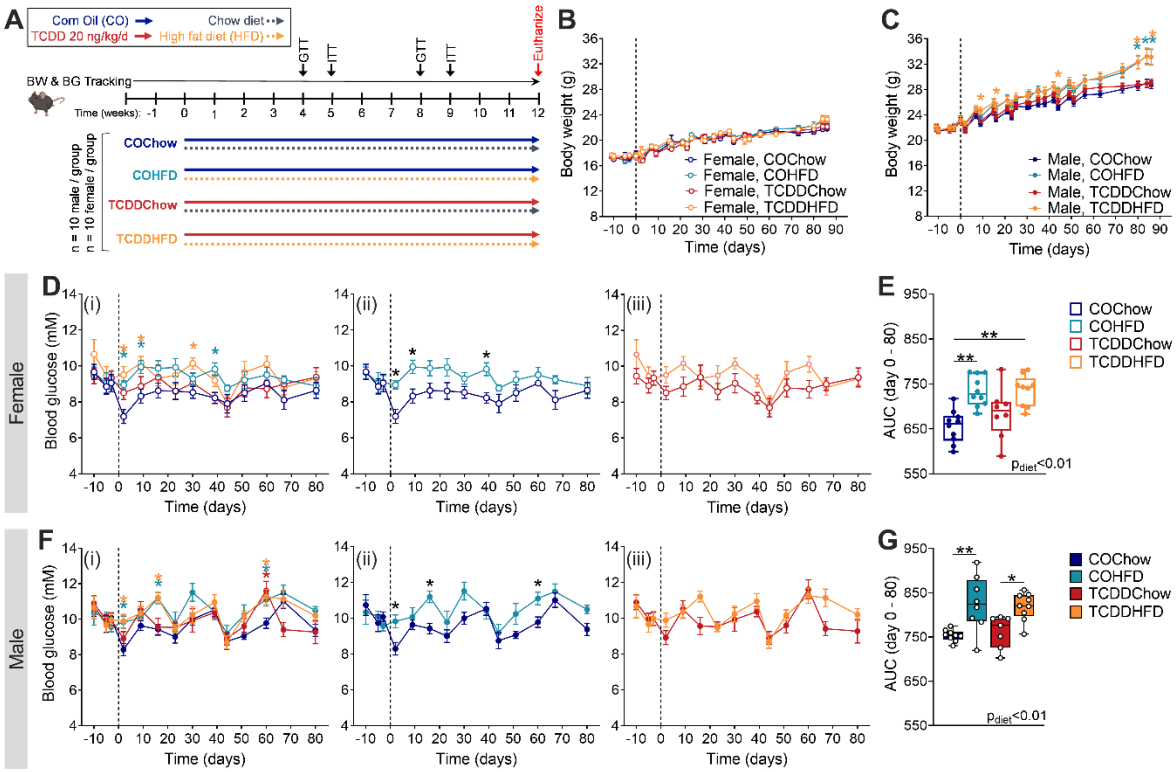

Fig. 1 Low-dose TCDD exposure does not impact body weight or fasting blood glucose levels in mice. (**A**) Male and female mice were exposed to corn oil or 20 ng/kg/d TCDD 2x/week for 12 weeks, and simultaneously fed either a chow diet or 45% HFD. Body weight and blood glucose was tracked throughout the 12-week study. BW = body weight; BG = blood glucose; GTT = glucose tolerance test; ITT = insulin tolerance test. (**B-C**) Body weight and (**D-G**) blood glucose were measured weekly following a 4-hour morning fast in (**B, D, E**) females and (**C, F, G**) males. (**D, F**) Blood glucose data are presented as (**i**) all groups compared to COChow, (**ii**) COHFD versus COChow, (**iii**) TCDDHFD compared to TCDDChow. Data are presented as mean ± SEM in line graphs or min/max values in box and whisker plots. Individual data points on box and whisker plots represent biological replicates (different mice). *p <0.05, **p <0.01, coloured stars are versus COChow. The following statistical tests were used: (**B, C, D, F**) two-way REML-ANOVA with Tukey's multiple comparisons test; (**E, G**) two-way ANOVA with Tukey's multiple comparisons test.

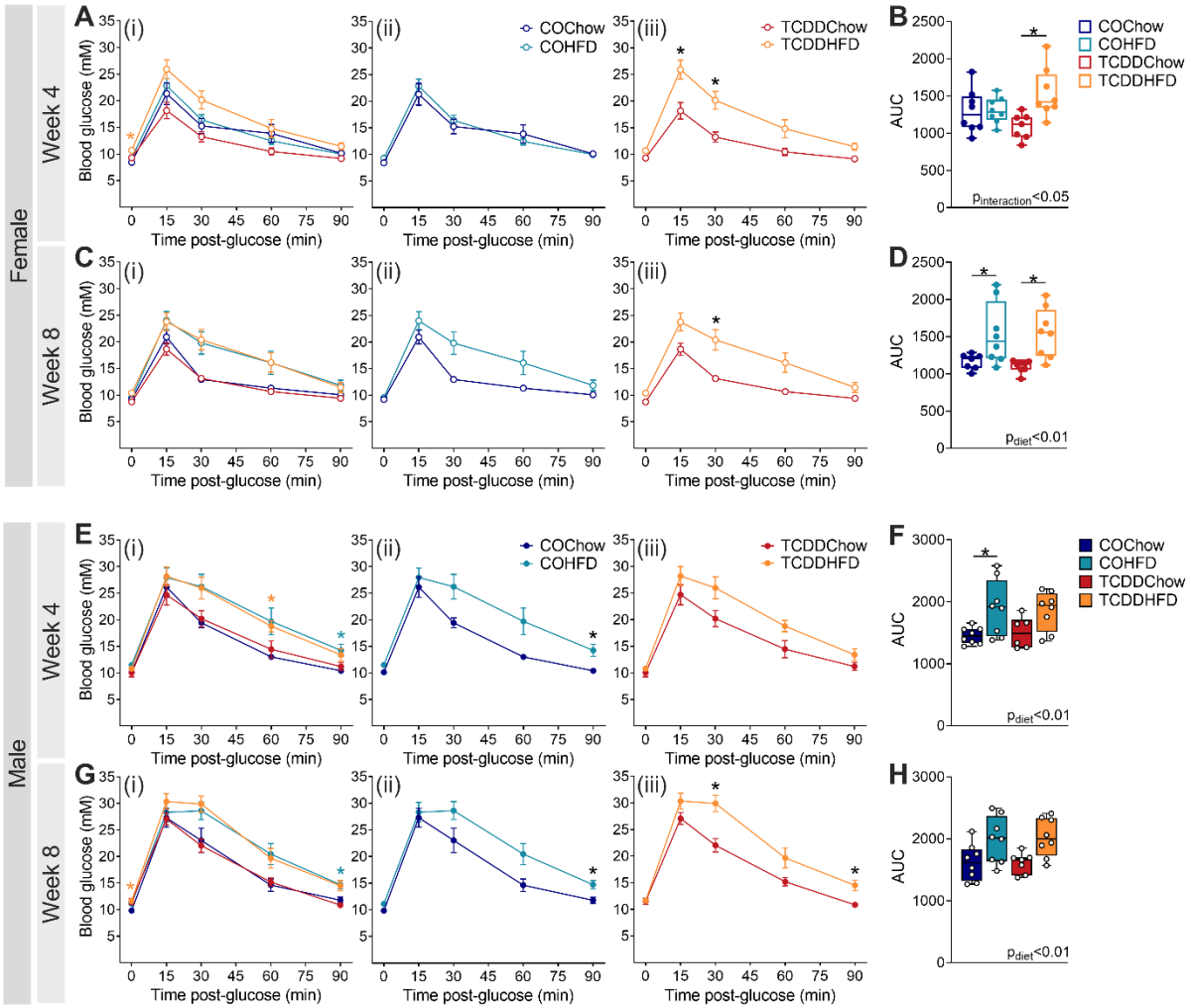

Fig. 2 TCDD exposure accelerates the onset of HFD-induced glucose intolerance in female mice. Glucose tolerance tests were performed after 4 and 8 weeks of TCDD exposure with/without HFD feeding (see **Fig. 1A** for study timeline). Blood glucose levels in (**A-D**) females and (**E-H**) males at (**A, B, E, F**) week 4 and (**C, D, G, H**) week 8. (**A, C, E, G**) Blood glucose data are presented as (**i**) all groups compared to COChow, (**ii**) COHFD versus COChow, and (**iii**) TCDDHFD compared to TCDDChow. Data are presented as mean ± SEM in line graphs or min/max values in box and whisker plots. Individual data points on box and whisker plots represent biological replicates (different mice). *p <0.05, coloured stars are versus COChow. The following statistical tests were used: (**A, C, E, G**) two-way RM ANOVA with Tukey's multiple comparison test; (**B, D, F, H**) two-way ANOVA with Tukey's multiple comparison test.

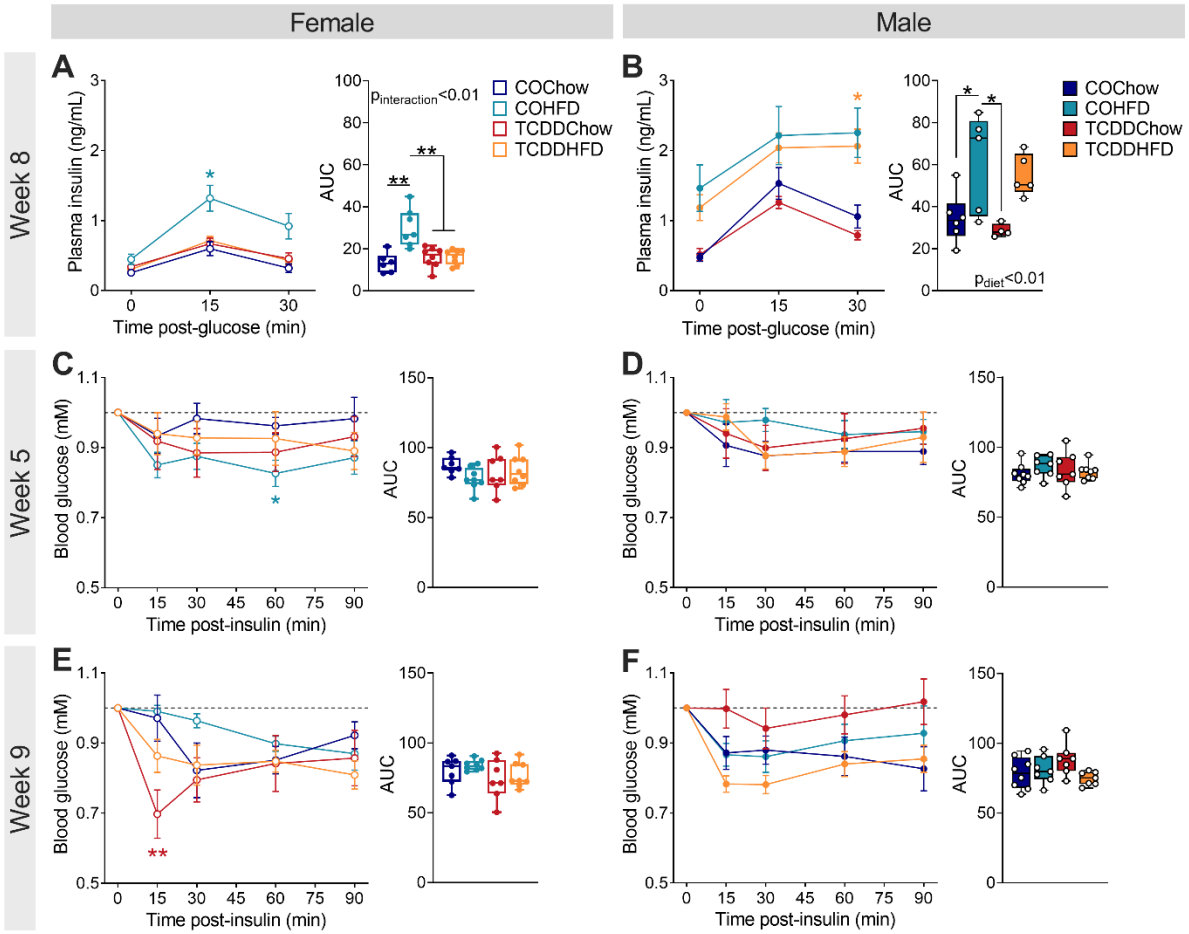

Fig. 3 TCDD-exposed female mice lack an appropriate compensatory hyperinsulinemic response to HFD feeding but had normal insulin tolerance. Glucose-stimulated plasma insulin levels were assessed *in vivo* at week 8, and insulin tolerance at week 5 and 9 (see **Fig. 1A** for study timeline). Plasma insulin levels during a GTT at week 8 of the study in (**A**) females and (**B**) males. Blood glucose levels during an ITT at (**C, D**) 5 weeks and (**E, F**) 9 weeks in (**C, E**) females and (**D, F**) males. Data are presented as mean ± SEM in line graphs or min/max values in box and whisker plots. Individual data points on box and whisker plots represent biological replicates (different mice). *p <0.05, **p <0.01, coloured stars are versus COChow. The following statistical tests were used: (**A-F**) line graphs, two-way RM ANOVA with Tukey's multiple comparison test; box and whisker plots, two-way ANOVA with Tukey's multiple comparison test.

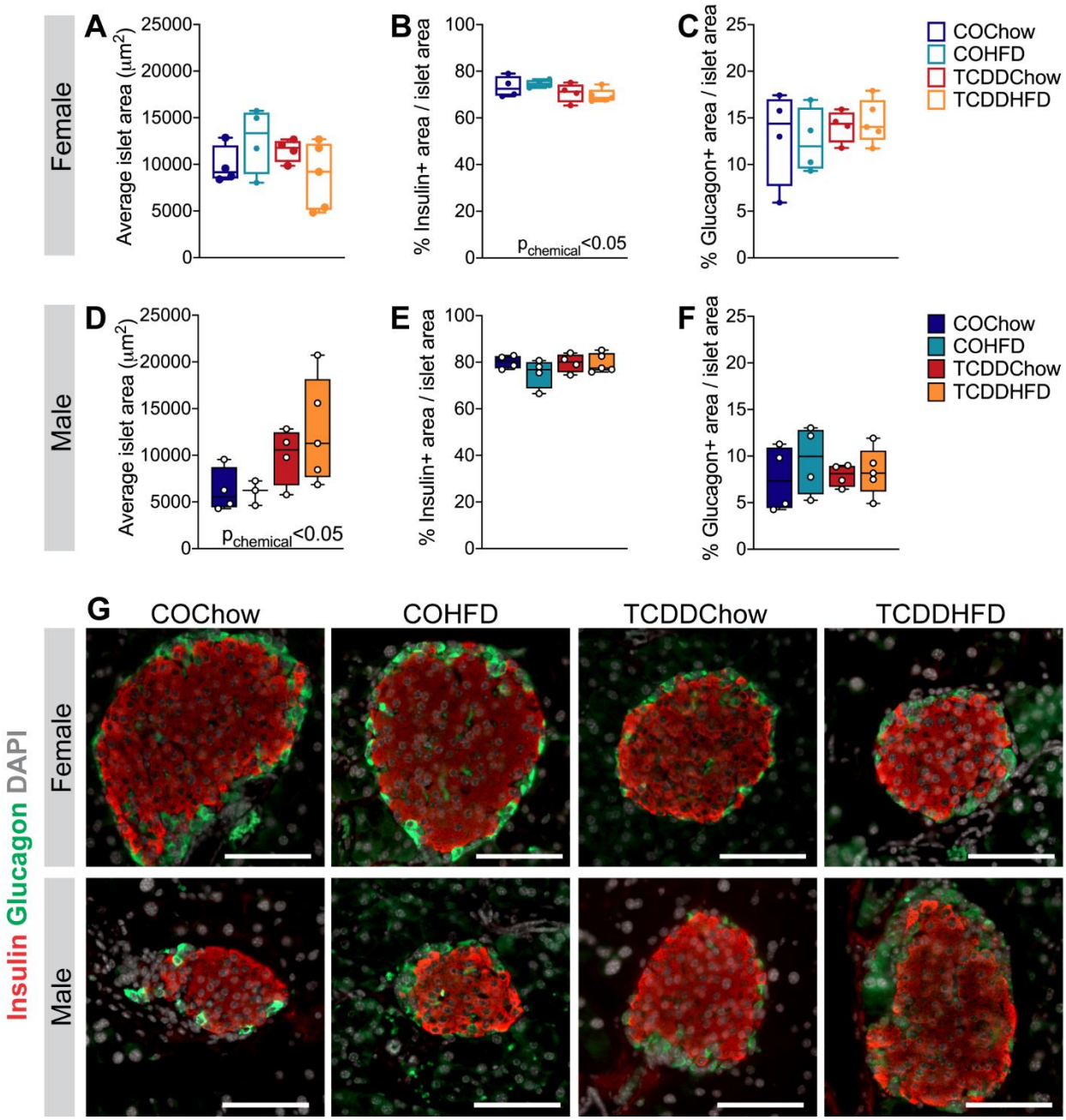

Fig. 4 Islet size and endocrine composition were unchanged by TCDD exposure. Whole pancreas was harvested at week 12 for analysis by immunofluorescence staining (see **Fig. 1A** for study timeline). (**A, D**) Average islet area, (**B, E**) % insulin^{+} area / islet area, (**C, F**) % glucagon^{+} area / islet area in (**A-C**) females and (**D-F**) males. (**G**) Representative images of pancreas sections showing immunofluorescence staining for insulin and glucagon. Scale bar = 100 µm. All data are presented as box and whisker plots with median and min/max values. Individual data points on box and whisker plots represent biological replicates (different mice). The following statistical tests were used: two-way ANOVA with Tukey's multiple comparison test.

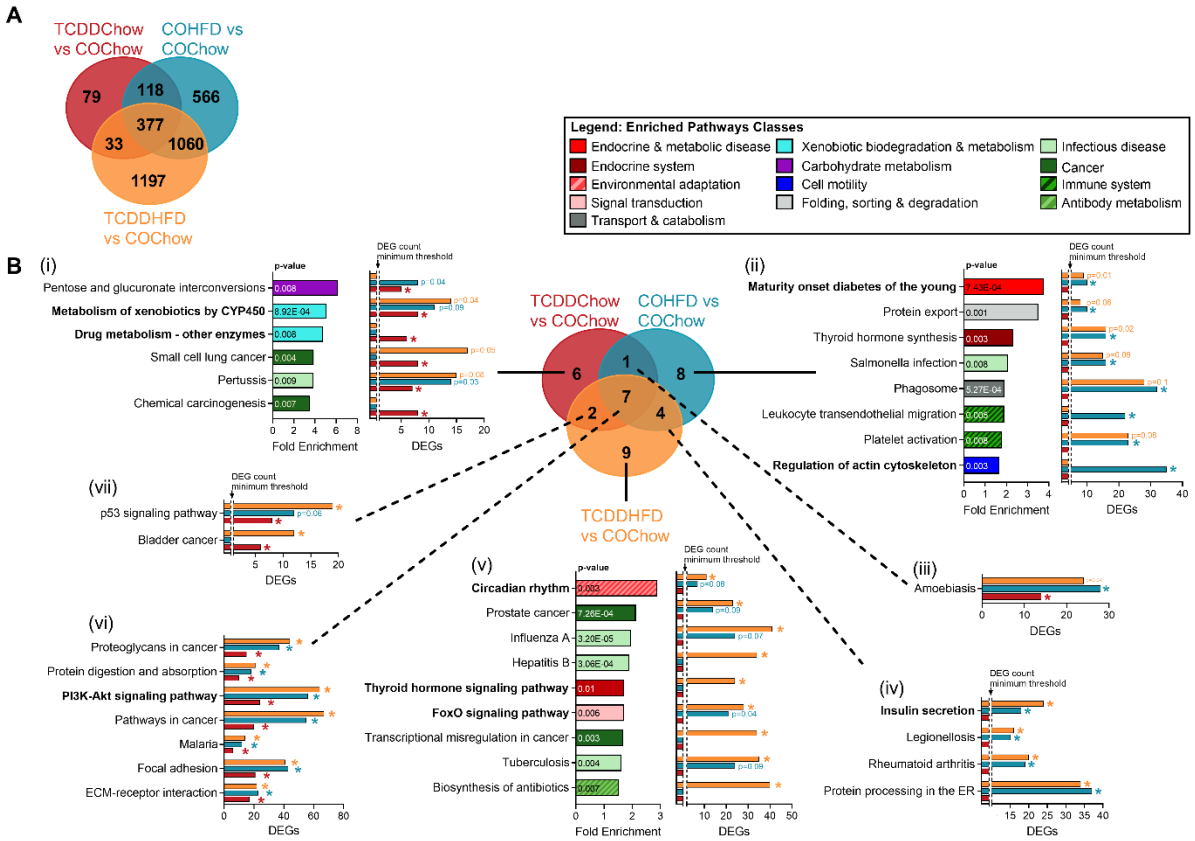

Fig. 5 TCDDHFD female mice have enriched endocrine-related pathways relative to COChow females. Islets were isolated from females at week 12 of the study for TempO-Seq® analysis (n=3-4/group). (**A**) Venn diagram displaying differentially expressed genes (DEGs) (adjusted $p < 0.05$, absolute fold change ≥ 1.5) in all experimental groups relative to COChow females. (**B**) KEGG pathway analysis was performed on all DEGs for each experimental group shown in (**A**). Results are displayed as a Venn diagram to show pathway overlap between experimental groups. For specific pathways, bar graphs show pathway fold enrichment in each group relative to COChow (DAVID modified Fisher Extract p-value < 0.01 relative to COChow females), and differentially expressed gene counts for statistically enriched pathways (coloured * = modified Fisher Extract p-value < 0.01 versus COChow). Pathways that were not trending or statistically enriched are indicated on bar graphs as not having the DEG count minimum threshold for significance.

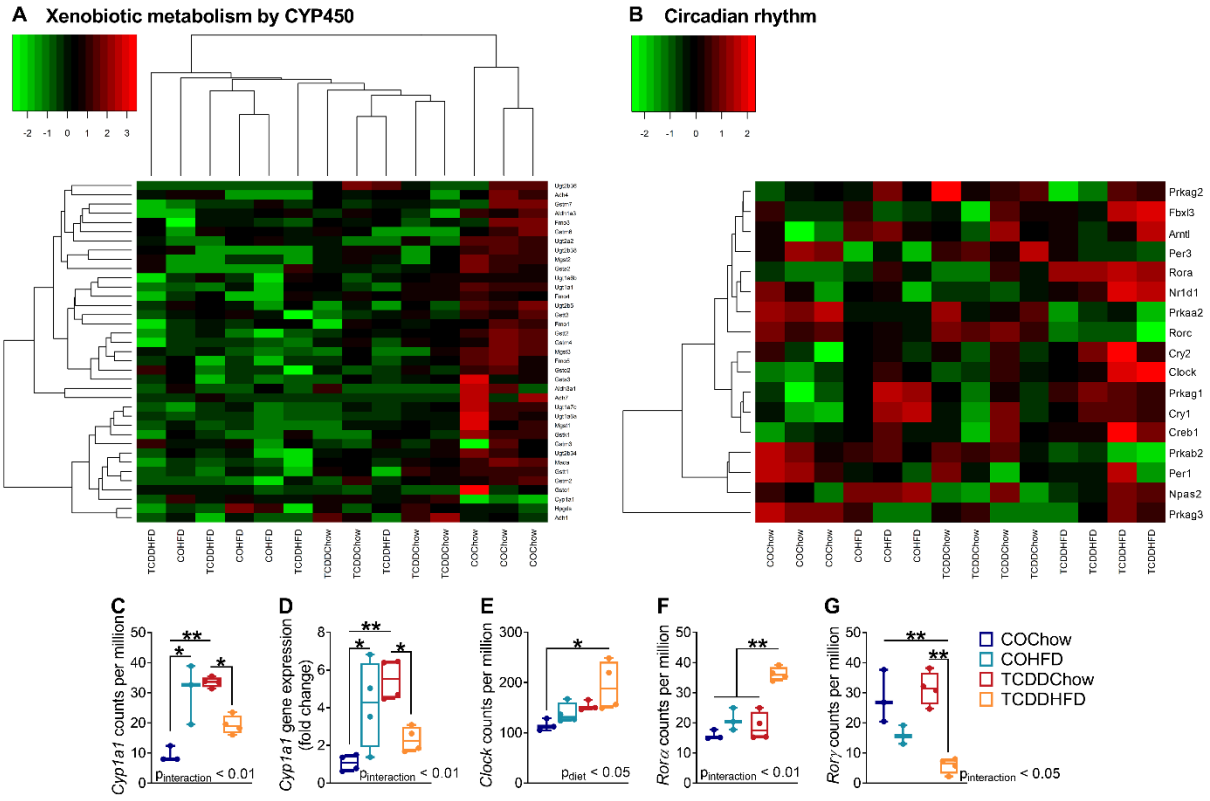

Fig. 6 TCDDHFD females have inappropriate Cyp1a1 and circadian rhythm gene expression. Islets were isolated from females at week 12 of the study for TempO-Seq® and qPCR analysis (n=3-4/group). (**A**) Hierarchal heatmap showing expression of genes involved in the "Xenobiotic Metabolism by CYP450" pathway. (**B**) Heatmap arranged by experimental group showing expression of genes involved in "Circadian Rhythm". (**C, E-G**) Gene expression of (**C**) *Cyp1a1*, (**E**) *Clock*, (**F**) *Rorα*, and (**G**) *Rorγ* in counts per million measured by TempO-Seq® analysis. (**D**) *Cyp1a1* gene expression measured by qPCR analysis. Individual data points on box and whisker plots represent biological replicates (different mice). All data are presented as median with min/max values. *p <0.05, **p <0.01. The following statistical tests were used: (**C-G**) two-way ANOVA with Tukey's multiple comparison test.

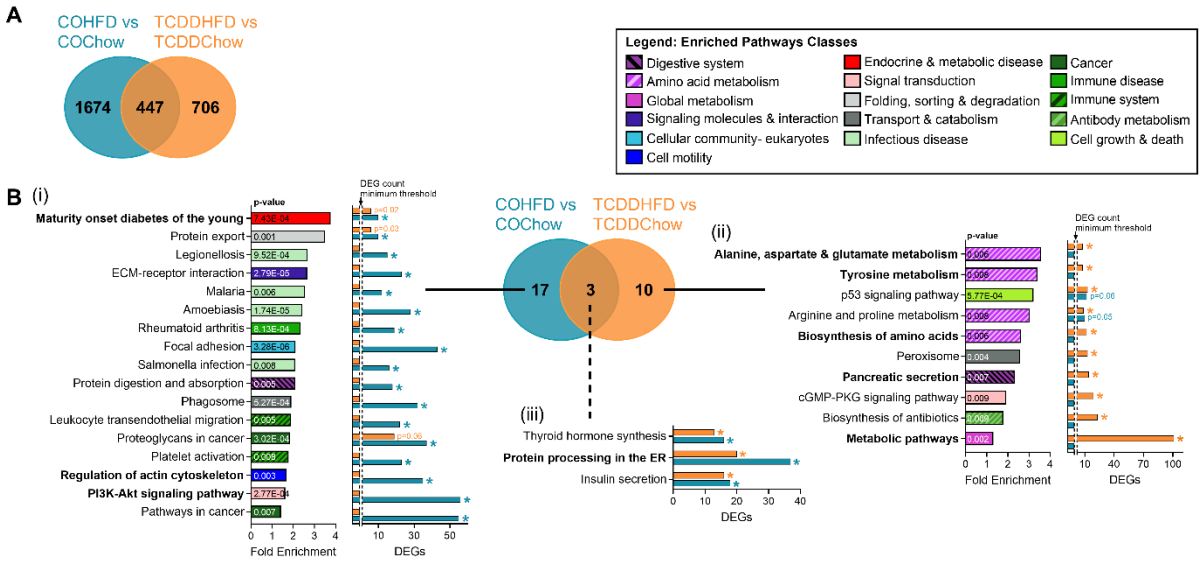

Fig. 7 TCDD exposure promotes HFD-induced changes in amino acid metabolism genes in islets. Islets were isolated from females at week 12 of the study for TempO-Seq® analysis (n=3-4/group). (**A**) Venn diagram displaying differentially expressed genes (DEGs) (adjusted $p < 0.05$, absolute fold change ≥ 1.5) in HFD fed females relative their respective chow-fed control female. (**B**) KEGG pathway analysis was performed on all the DEGs for each comparison shown in (**A**). Results are displayed as a Venn diagram to show pathway overlap between experimental groups. For specific pathways, bar graph show pathway fold enrichment in each HFD-fed groups with respect to their chow-fed control (DAVID modified Fisher Extract p-value < 0.01 relative to respective chow-fed control), and differentially expressed gene counts for statistically enriched pathways (coloured * = modified Fisher Extract p-value < 0.01 versus chow-fed control). Pathways that were not trending or statistically enriched are indicated on bar graphs as not having the DEG count minimum threshold for significance.

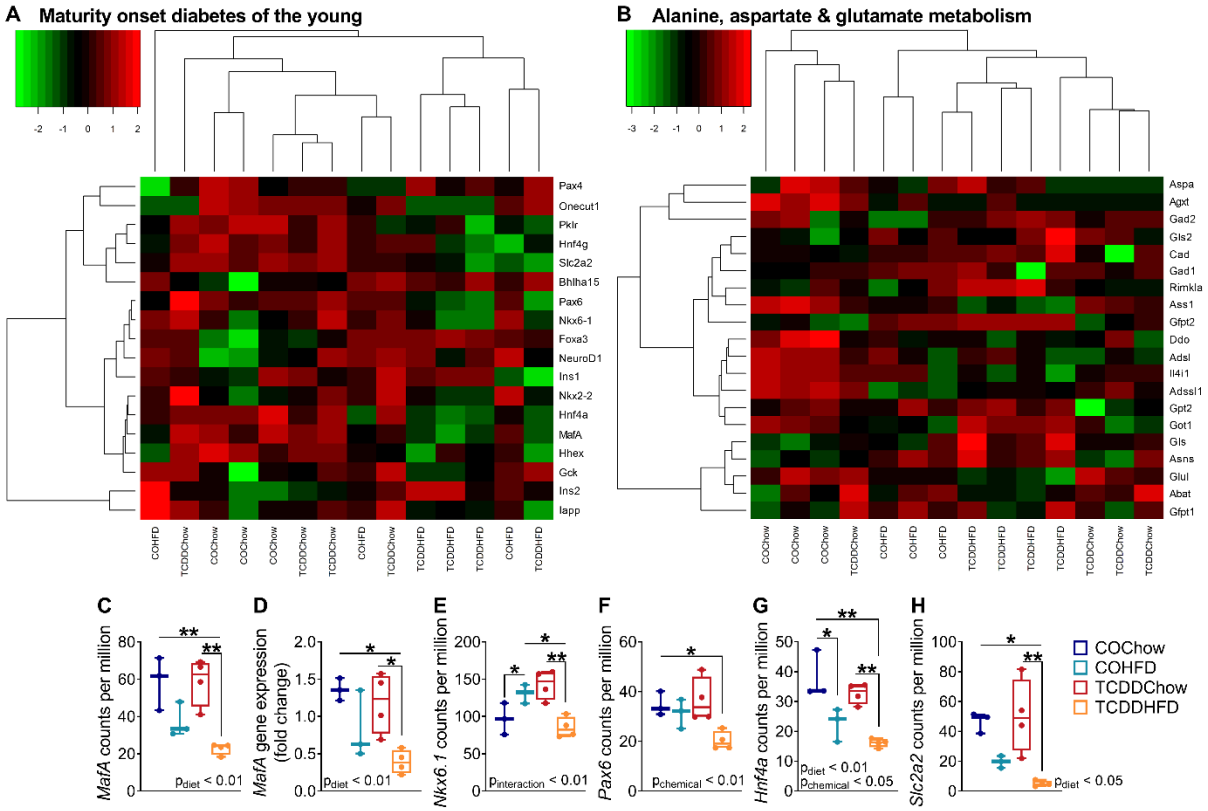

Fig. 8 TCDD promotes HFD-induced changes in MODY and alanine, aspartate, and glutamate metabolism gene expression. Islets were isolated from females at week 12 of the study for TempO-Seq® and qPCR analysis (n=3-4/group). (**A-B**) Hierarchical heatmaps showing expression of genes involved in (**A**) "Maturity Onset Diabetes of the Young" and (**B**) "Alanine, Aspartate and Glutamate Metabolism". (**C, E-H**) Gene expression of (**C**) *MafA*, (**E**) *Nkx6.1*, (**F**) *Pax6*, (**G**) *Hnf4α*, and (**H**) *Slc2a2* in counts per million measured by TempO-Seq® analysis. (**D**) *MafA* gene expression measured by qPCR analysis. Individual data points on box and whisker plots represent biological replicates (different mice). All data are presented as median with min/max values. *p <0.05, **p <0.01. The following statistical tests were used: (**C-H**) two-way ANOVA with Tukey's multiple comparison test.